Materials and Design 190 (2020) 108595

Contents lists available at ScienceDirect

Materials and Design

journal homepage: www.elsevier.com/locate/matdes

Shear punching of bulk metallic glasses under low stress

Fei Sun [a,b], Bei Wang [a], Feng Luo [a], Yu Qiang Yan [b], Hai Bo Ke [b,*], Jiang Ma [a,*], Jun Shen [a], Wei Hua Wang [b]

[a] College of Mechatronics and Control Engineering, Shenzhen University, Shenzhen, People's Republic of China
[b] Songshan Lake Materials Laboratory, Dongguan, People's Republic of China

HIGHLIGHTS

- The ultrasonic assisted shear punching of BMGs is proposed.
- The advantages of the proposed punching are demonstrated.
- The ultrasonic assisted punching requires 1/10 stress of the traditional theory.
- A phenomenological ultrasonic softening mechanism of BMG is proposed.

GRAPHICAL ABSTRACT

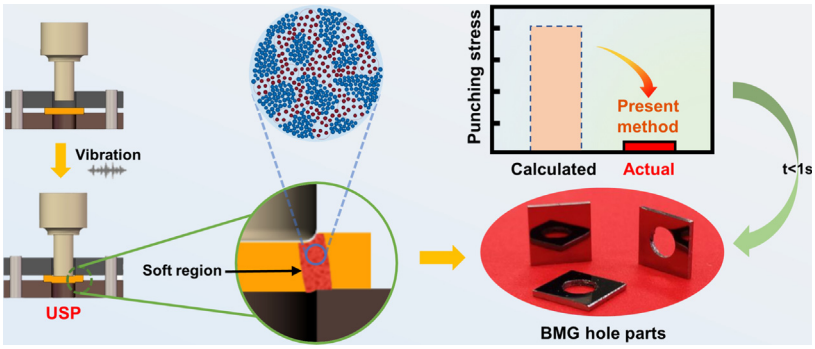

ARTICLE INFO

Article history:
Received 4 November 2019
Received in revised form 19 February 2020
Accepted 20 February 2020
Available online xxxx

Keywords:
Punching
Ultrasonic vibration
Bulk metallic glasses
Cyclic liquefaction

ABSTRACT

Bulk metallic glasses (BMGs) possess excellent mechanical properties yet poor efficient processing ability at room temperature which limits the application of BMGs. Here, we report a high efficiency and energy-saving punching method suitable for processing of BMGs. By use of ultrasonic vibration on the punch, the accurate shape can be quickly manufactured from a BMG plate with a thickness upon 1 mm at an extremely low punch pressure of 110 MPa, which is less than one tenth of the estimated value by conventional theory. The underline physical mechanism of softening in BMG during the ultrasonic vibration assisted punching process was interpreted by cyclic liquefaction or the activation and connection of liquid-like regions in the elastic matrix of BMGs. This work would provide a novel route for solving the machining problem of BMGs at room temperature and promote wider applications of BMGs in precision manufacturing field.

1. Introduction

Owing to the unique disordered structure, the mechanical properties of BMGs tend to be superior compared with their metallic counterparts, such as higher strength and hardness, better wear resistance [1–6]. Therefore, BMGs have been considered to be the promising structural materials in the next generation [7–10]. However, BMGs exhibit macroscopic brittleness during deformation, which seriously hinders their application as structural materials. Once the stress exceeds its yield strength, the formation, propagation and penetration of shear bands throughout the samples will lead to the catastrophic failure of BMGs [11–13]. This mean that the conventional processing methods based on deformation of the material are not applicable for BMGs. The brittle nature of BMGs acts as Achilles' heel and restricted these materials to form into useful products. A compromising method is the thermoplastic forming for BMGs [14,15]. When the temperature reaches the glass transition temperature, the metallic glass enters the

* Corresponding authors.
E-mail addresses: khb0304@163.com (H.B. Ke), majiang@szu.edu.cn (J. Ma).

https://doi.org/10.1016/j.matdes.2020.108595

supercooled liquid state and has super plasticity [16,17]. However, the metastable state of BMGs leads to a high risk of crystallization during this process, which limits the potential applications of thermoplastic forming of BMGs. Therefore, it is urgent to have novel processing techniques suitable for their room temperature processing and promote the application of BMGs.

Shear punching is an effective forming technology for traditional metals or plastics [18]. The shear punching has also been applied to MG sheets or strips with thickness only in the order of several micrometer [19–23]. Qiao et al. established a correlation between the maximum shear punched thickness and shear strengths for various BMGs [24]. However, due to the high strength and inherent brittleness, the larger stress is required once a larger thickness of MG is punched, resulting in lower processing efficient and higher cost. So, the question is then raised: Is it possible to using a lower stress for processing of BMGs? It is known that the MGs were composed of liquid-like regions and elastic solid-like regions [25–28]. These liquid-like regions may grow or reconfigure themselves according to the external condition including loading or temperature rising, which was considered to be responsible for the deformation or glass transition behavior [25–27,29,30]. It had also been proved that ultrasound loading can activate these regions and cause local softening of MGs [28]. Thus, proper introduction of ultrasonic technology can reduce the processing stress of BMGs.

In this work, we firstly bring cold forming concept and technology into BMGs by proposing a high efficient low-stress ultrasonic-vibration-assisted shear punching (USP) method. Using of this approach, accurate shape can be quickly manufactured within 1 s on a BMG plate with a thickness upon 1 mm with a stress less than one tenth of its strength. Our results show that the brittle nature of BMGs could be bypassed and specific shapes could be formed under room temperature. This high efficient and low cost forming method will provides a novel route for the processing of BMGs and throw light on their extensive engineering applications.

2. Experimental procedures

The conventional $Zr_{50.5}Al_9Ni_{13.05}Cu_{27.45}$ (at.%) BMGs with a thickness of 1 mm were chosen for the present work. The alloy ingots were prepared by arc melting a mixture of elements with a purity at least 99.9% under a Ti-gettered purified Ar atmosphere. To ensure a homogeneous composition, each ingot was remelted five times. Afterwards metallic glass plates with a dimension of 1 mm × 20 mm × 50 mm were obtained by casting the molten alloy into a copper die. The tensile strength of the BMG plate was determined to be 1500 MPa by tensile test, which is consistent with previous literature [31]. In addition, several typical crystal materials with a thickness of 1 mm were chosen for comparison, including phosphor copper, spring steel and stainless steel, which was purchased directly from commercial suppliers. For the convenience, the workpieces were cut into a square with a dimension of 10 mm × 10 mm by a low-speed wire electrical discharge machining (WEDM; SODICK AP250L).

The glassy nature of the samples before and after punching was ascertained by the X-ray diffraction (XRD; Rigaku MiniFlex 600) with Cu K_α radiation and differential scanning calorimetry (DSC; Perkin–Elmer DSC-8000) at a heating rate of 20 K/min. The micro morphologies and elemental distributions of samples were characterized by LYRA3 FIB-SEM scanning electron microscope (SEM) instrument, and FEI Titan Cubed Themis G2 300 transmission electron microscope (TEM) equipped with energy disperse spectroscopy (EDS). The TEM sample was prepared by the FEI Scios focused ion beam/scanning electron microscope (FIB/SEM) system.

A schematic diagram of shear punching and forming processes of USP is depicted in Fig. 1. The intelligent ultrasonic generator generates the initial ultrasonic signal with a frequency of 20 kHz. The transducer converts ultrasonic signal into mechanical vibration, then through the amplification of the ultrasound horn, the ultrasonic punch obtains final high-frequency mechanical vibration, as shown in Fig. 1(a). The forming processes of workpiece including BMGs as well as crystalline alloys are shown in Fig. 1(b-d). The workpiece was placed above the die equipped with a positioning frame of 10.1 mm × 10.1 mm in square and 0.2 mm in depth. The workpiece was pressed using a pressure plate and a bolt, the ultrasonic vibration and pressure are transmitted to the workpiece when the ultrasonic punch is lowered. The ultrasonic punch is made of cemented carbide (TC4 titanium alloy in present work) with a tip diameter of 5 mm.

3. Results and discussion

3.1. Comparison with typical crystalline alloys

For crystalline materials, the pressure required to complete shear punching is expressed by the following equation [32]:

$$P = \frac{4T\sigma}{d} \tag{1}$$

where P, T, σ and d are the required punching pressure, workpiece thickness, tensile strength of workpiece material and diameter of die, respectively. The thickness of workpieces are all 1 mm and the tensile strength of BMG is 1500 MPa as shown in Fig. 2(a). The diameter of the die is 5 mm. According to Eq. 1, the required punching pressure P of MG plate is 1200 MPa. However, the actual applied pressure is only 110 MPa, which is less than one tenth of the calculated theoretical value. Fig. 2(b) schematically draws the relationship between theoretical stress of the workpiece under the traditional mechanism and the actual stress of the MG plate using the USP. Obviously, the traditional deformation mechanism does not apply to MG during USP.

Several typical crystalline materials including stainless steel, spring steel and phosphor copper with various tensile strengths were selected to USP for comparison. The tensile strength of these materials is 900 MPa, 650 MPa and 500 MPa, as shown in Fig. 2 (a), respectively. According to Eq. (1), the pressure required to complete the shear punching of stainless steel, spring steel and phosphor copper is 720 MPa, 520 MPa and 400 MPa, respectively. For comparison, the pressure of 72 MPa, 52 MPa and 40 MPa, which equal to one tenth of the stress required to shear the crystalline materials were applied to stainless steel, spring steel, phosphor copper, respectively.

As shown in the left column of Fig. 3(c), the highest strength stainless steel plate did not undergo any deformation, the spring steel plate with the second large strength shows slight bending, even the copper with the lowest strength was plastically deformed merely. We also applied the same stress of the BMG plate during the USP to the three crystalline materials, as shown in the right column of Fig. 3(c), the stainless steel is only slightly bent, the spring steel is plastically deformed, the copper plate with a strength of one-third of the metallic glass is only shear-deformed instead of being punched out. Obviously, the crystalline materials with much lower strength than BMG cannot be punched out using USP. The remarkable contrasts indicate that the BMG underwent a completely different deformation mode in contrast to that of traditional metals during the ultrasonic vibration assisted shear punching process. In fact, by using a similar method, we have obtained a variety of complex parts of metallic glass in our previous papers, such as English letters [22], stator core and other Special-shaped hole parts with complicated contours [28]. Those results indicated that the method was feasible for the complex shaping of metallic glass ribbons. As for the bulk sample with thickness more than 1 mm, hole punching is a basic cold forming process for traditions metals, this simple process being successfully realized is a prerequisite the complex shapes or parts could be formed in BMGs. That is the reason we choose to do the hole punching firstly. However, the ultrasonic vibration machine needs to be redesigned to accomplish complex shapes or parts punching, including the power adjustment, sonotrode redesign, mold adaptation *et al*, which

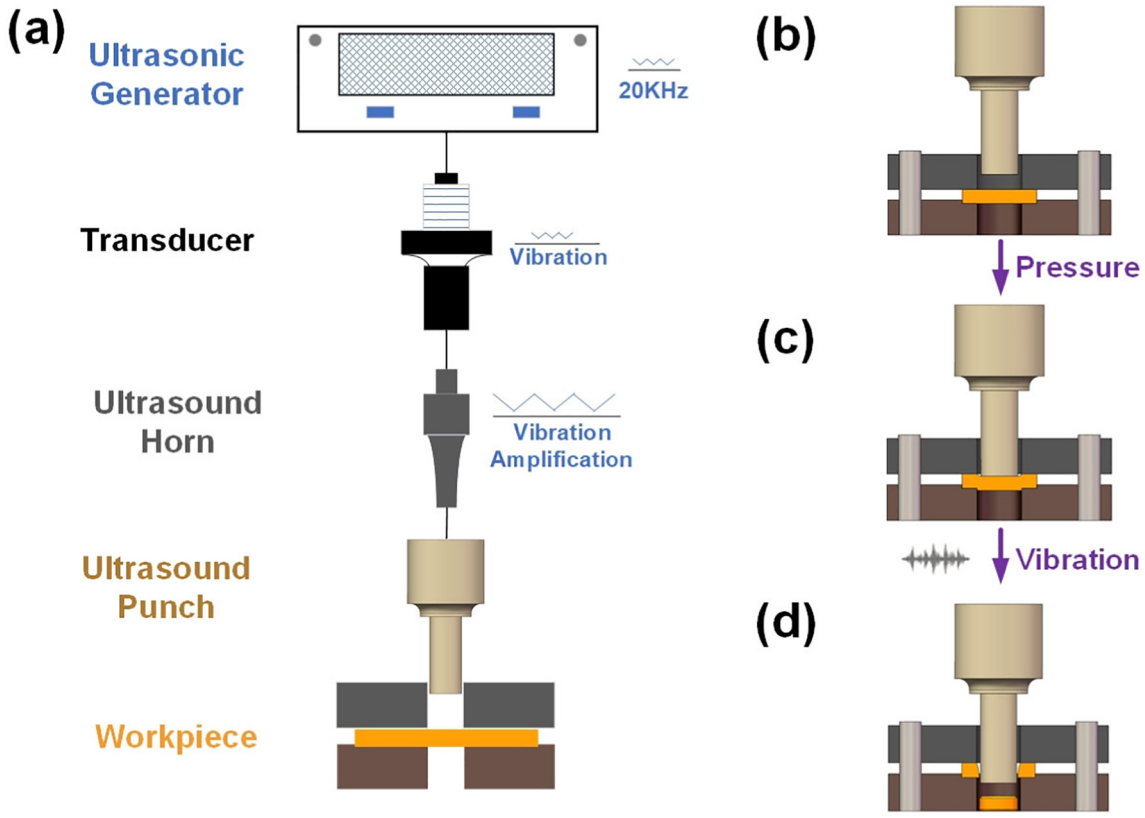

Fig. 1. (a) Illustration of the USP method for workpiece of BMGs and crystalline alloys. (b-d) The forming processes of USP.

is a complex project to be done and we are trying to continue in the next phase of this research.

3.2. Characterization

The Zr-based BMG samples before and after the USP were tested by XRD and DSC. The experimental results are displayed in Fig. 4. As shown in Fig. 4(a), the XRD pattern of BMG specimen after punching shows the same halo profile without change. The DSC curve in Fig. 4(b) also confirms the amorphous nature after shear punching and the crystallization enthalpy before and after punching are almost unchanged.

The micro- and atomic-structure of the edge portion of the hole and the center portion of the disc, as shown in Fig. 4(b), were examined. Fig. 4(d)and (f) show the high-resolution electron micrographs and diffraction pattern of the selected area under the transmission electron microscopy (TEM), respectively. As can be seen, the amorphous structure and the obvious halo rings indicate that the region experienced the most severe deformation still maintains the amorphous nature. In addition, the element distribution examined by the energy dispersive spectroscopy (EDS) shown in Fig. 4 (d) and (e), reveals that ultrasonic vibration did not change the element composition and distribution after punching.

3.3. Section morphology

The fracture morphology near the edges of circle after USP was conducted. The typical cross-section was presented in Fig. 5(a), the magnification of the selected rectangle area was displayed in Fig. 5(b). One can see that the dimples with wire-like margin appearance is formed and distributed evenly throughout the section. The average size of the

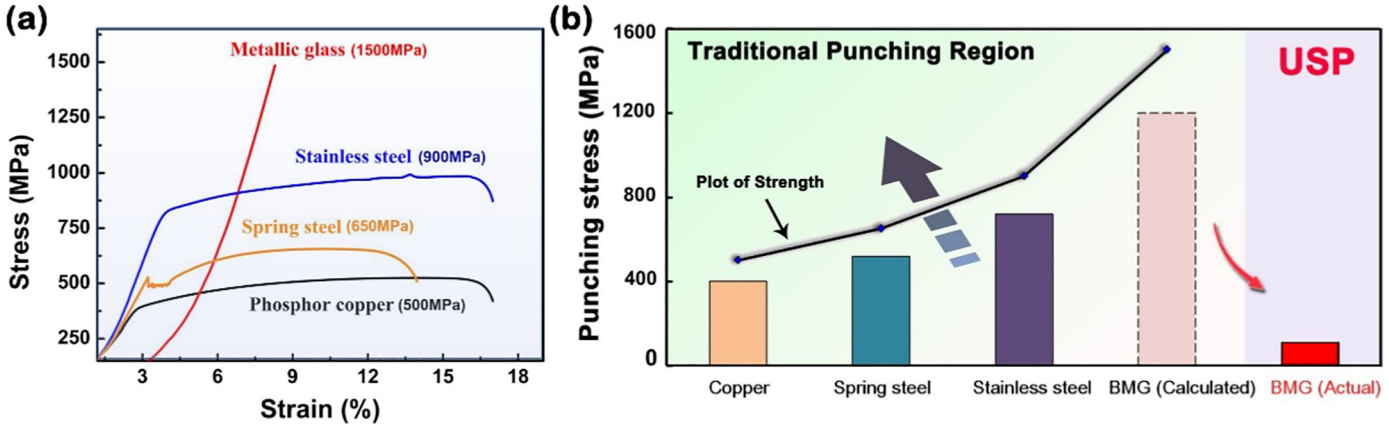

Fig. 2. (a) Tensile curve of the selected material. (b) Comparison of theoretical punching stress (represent by the pillar) and actual stress of the MG plate during the USP, the tensile strength of these materials has also been plotted.

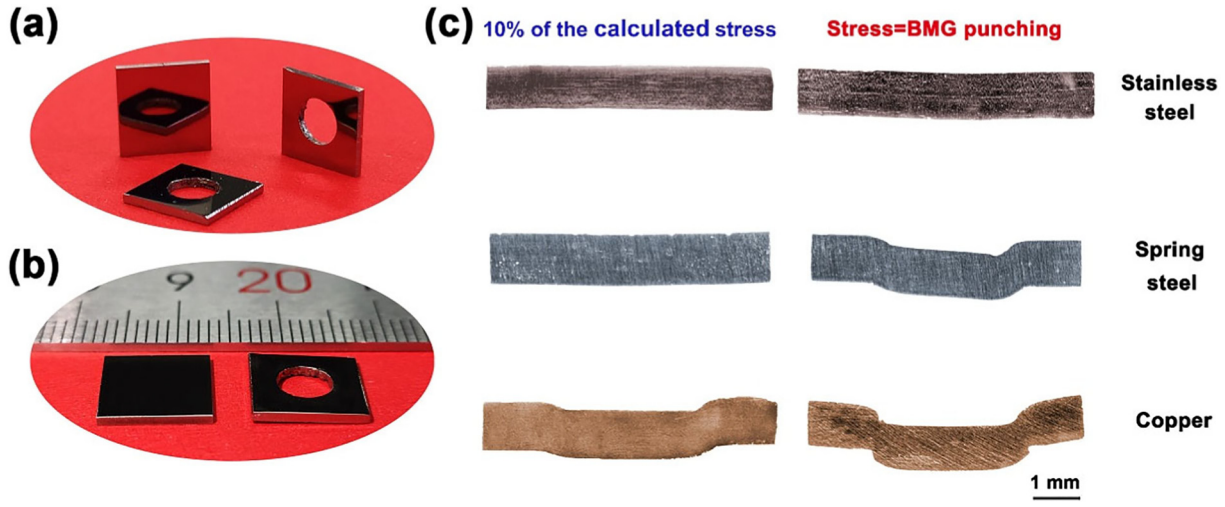

Fig. 3. (a, b) The different perspectives of MG plate and samples after USP. (c) Left column:deformation of crystalline materials under one tenth of the calculated stress. Right column: deformation of crystalline materials under the equal stress to BMG.

dimples is more than a dozen microns. The wire-like margin appearance means that a Newtonian-flow behavior occurred during the torn apart process of MG [33]. For comparison, the cross-section of a compressed Zr-based BMG sample was also presented in Fig. 5(c), the inset shows the overall fracture angle under normal compression. In general, BMG under compressive stress will store elastic energy until a very high value is reached, then the local shear bands initiate and lead to the typical vein-like pattern as shown in Fig. 5(c). Obviously, the fracture

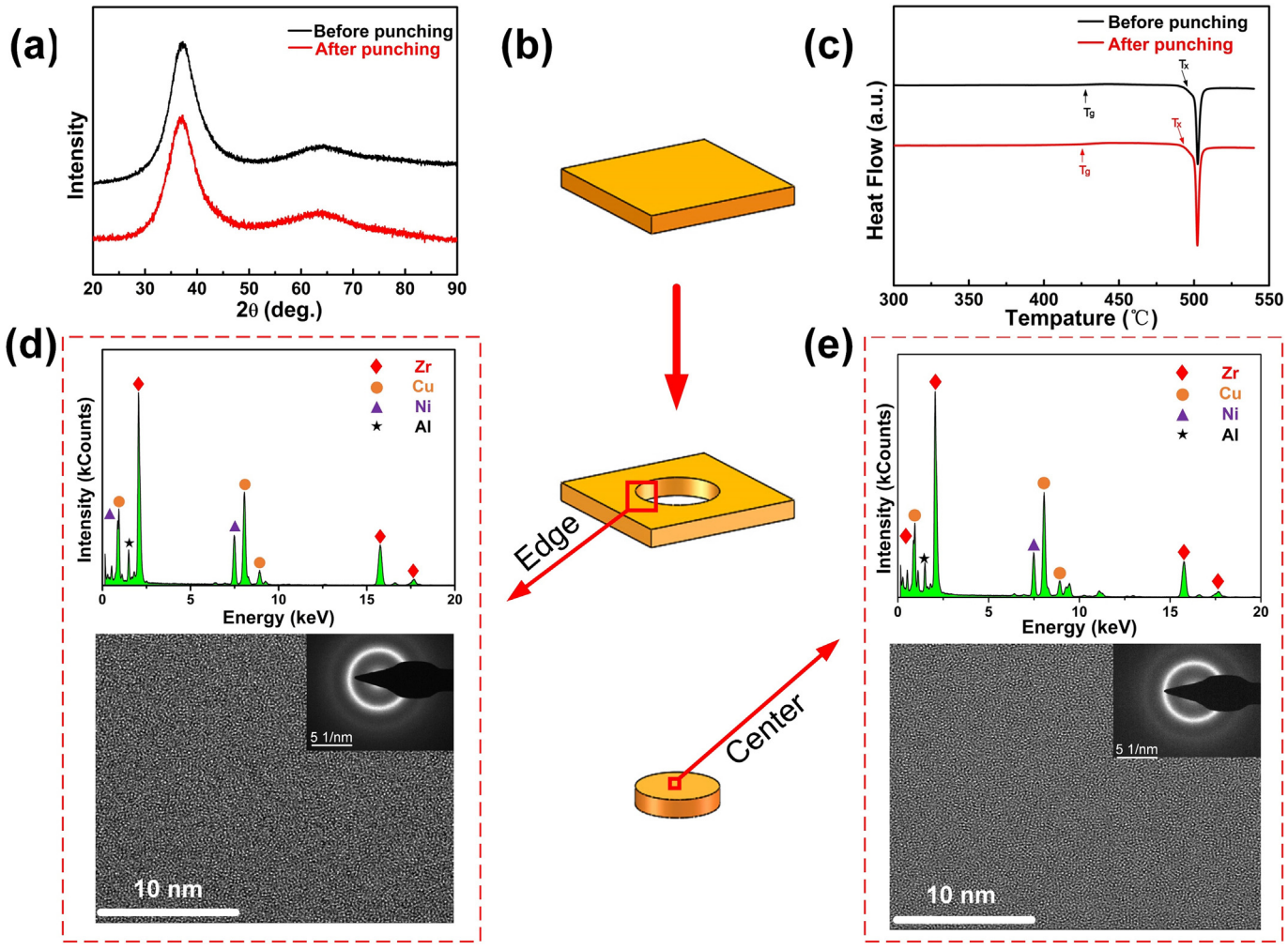

Fig. 4. (a) Comparison of XRD results before and after the USP. (b) BMG plate before USP, hole parts and disc parts. (c) Comparison of DSC results before and after the USP. (d) Characterization of the edge portion of the hole part. (e) Characterization of the central portion of the disc.

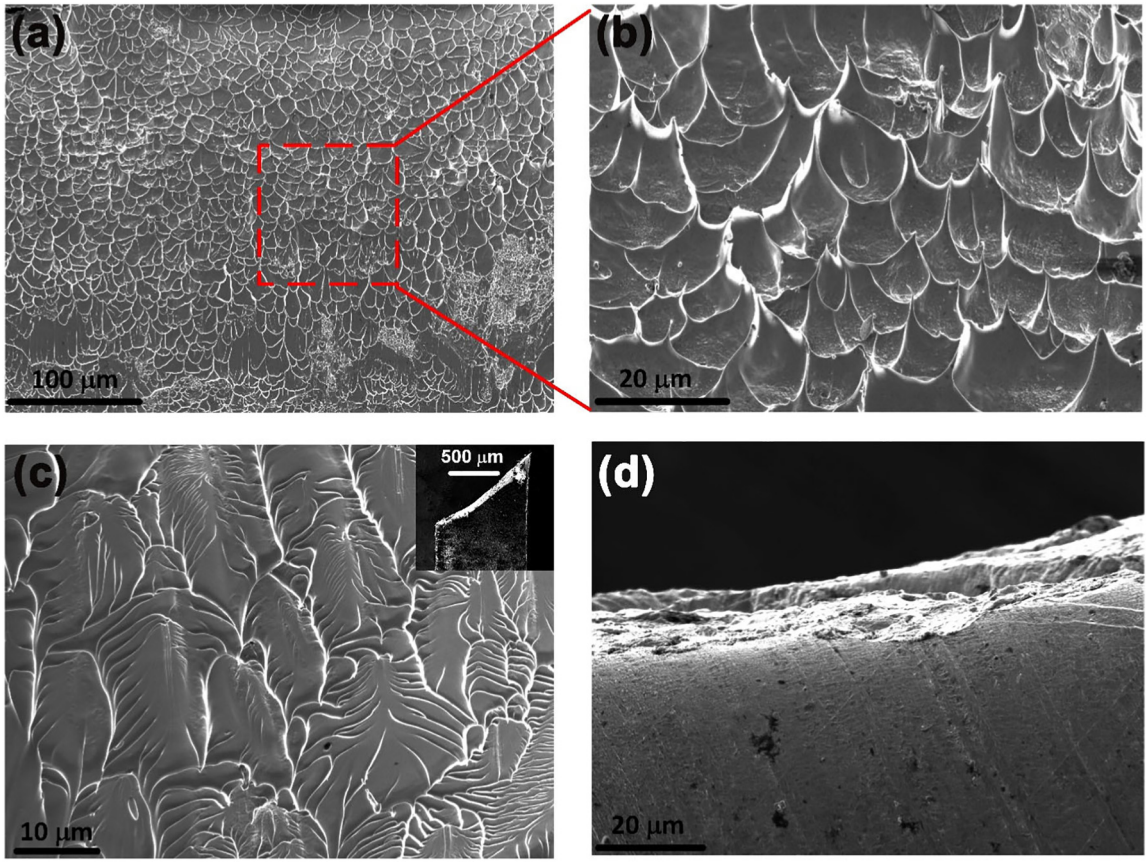

Fig. 5. (a) The fracture morphology of MG after USP. (b) The magnification of the selected red rectangle area. (c) The fracture morphology of the compressed BMG sample, the inset shows the overall fracture angle under normal compression. (d) The edge morphology of hole parts for MG sample after USP. (For interpretation of the references to colour in this figure legend, the reader is referred to the web version of this article.)

morphology of the USP sample had a significant difference with the compressed sample. This striking contrast means that the USP fracture has a different mechanism compared with conventional compressive brittle fracture. Fig. 5(d) shows the edge of the punched hole, almost no shear band can be found. Normally, the traditional shear punching process applied to amorphous alloys inevitably cause a large number of shear bands at the edges of the holes [34].Thus, the uncontrollable shear bands behavior was suppressed during USP process, which is the activated shear flow that caused the punching of BMG under such a low stress at room temperature.

3.4. Mechanism

A phenomenological model of cyclic liquefaction was proposed to understand the underlying mechanism of USP. It is known that cyclic loading of a saturated or partially saturated soil will cause a loss of the strength and stiffness [35,36], which was termed as cyclic liquefaction. Actually, MG is regarded to have an analogous microstructure with saturated soil [37,38], and MGs comprise liquid-like and solid-like regions, similar to the solid soil and liquid water in the saturated or partially saturated soil. The solid-like regions percolate to form an elastic network while the liquid-like ones encaged in network acts as viscous flow units for energy dissipation (as shown in Fig. 6(a)). Shear induced dilatation has been extensively studied in randomly packed structures, such as soils and granular media [39,40], and in the deformation of MGs [41,42]. Large increases in volume associated with local shearing events can occur even in the elastic region for MG, which is beneficial to the growth and generation of liquid-like region [43–45]. Under the external force, the liquid-like regions in MGs can be activated and extended, causing the increase of their fraction [25]. In our case, even the applied stress is only one of tenth of the MG's strength, nevertheless, the assistant high frequency ultrasound vibration could significantly amplify above effect. With the increase of vibration time, the extended liquid-like regions connected together as a whole, the BMG sample would exhibit viscous behavior and flow, resulting in the punching off. The schematic diagram of cyclic liquefaction behavior in MG during USP process is displayed in Fig. 6. As one can see from Fig. 6(a) and (b), when enough liquid-like regions were activated and connected together, the interconnected elastic network would be damaged, and the strength and stiffness of the BMG can be greatly decreased, and BMG then becomes easily formed under the punch. According to our existing experimental data, the physical properties and thermal stability of BMG after high-frequency vibration loading are improved. After the punching process when the ultrasonic vibration stopped, the atoms would reduce their mobility in the liquid-like regions because of the removal of ultrasound excitation source, therefore, the connection of liquid-like regions would break and form new solid-like regions, resulting in solid state amorphous alloy, as one can see from Fig. 6(b) to (c).

4. Conclusion

In summary, a low stress ultrasonic-vibration-assisted shear punching approach for BMGs is proposed. By using of this method, an accurate circle BMG part can be obtained in less than 1 s. It should be noted that the processing stress is only one tenth of the traditional punching technology. The deformation mechanism of USP for BMG is novel and different from the traditional punching method, which is comprehended by cyclic liquefaction or the activation and connection of liquid-like regions in MG. The proposed method firstly brings cold forming concept and technology into BMGs. The method bypasses the

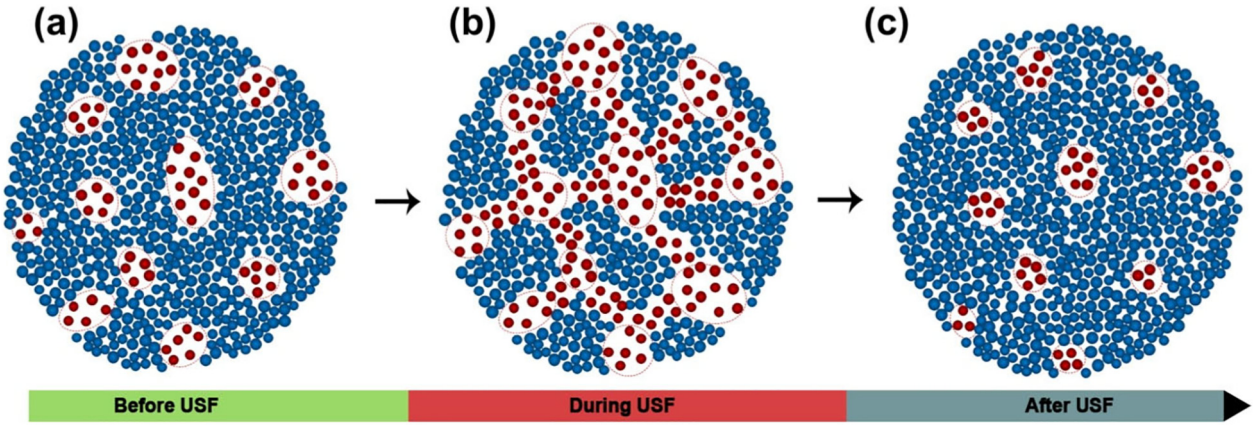

Fig. 6. The schematic diagram of cyclic liquefaction in MG during USP process.

brittle nature of BMGs and produces specific shapes under room temperature, which could promote their wider engineering application.

CRediT authorship contribution statement

Fei Sun: Conceptualization, Writing - original draft, Investigation.**Bei Wang:**Investigation.**Feng Luo:**Formal analysis.**Yu Qiang Yan:**Formal analysis, Resources.**Hai Bo Ke:**Supervision, Resources, Writing - review & editing.**Jiang Ma:**Supervision, Resources, Writing - review & editing. **Jun Shen:**Writing - review & editing.**Wei Hua Wang:**Writing - review & editing.

Declaration of competing interest

We declare that no conflict of interest exits in the submission of this manuscript, and manuscript is approved by all authors for publication. I would like to declare on behalf of my co-authors that the work described was original research that has not been published previously, and not under consideration for publication elsewhere, in whole or in part. All the authors listed have approved the manuscript that is enclosed.

Acknowledgements

The work was supported by the Key Basic and Applied Research Program of Guangdong Province, China (Grant Nr. 2019B030302010), the National Key Research and Development Program of China (Grant No. 2018YFA0703605), the National Science Foundation of China (Grant No. 51871157, 51775351), the Science and Technology Innovation Commission Shenzhen (Grants No. JCYJ20170412111216258), the National Natural Science Foundation of Guangdong Province (Grant No. 2017A030313311).

References

[1] W. Klement, R. Willens, P. Duwez, Non-crystalline structure in solidified gold-silicon alloys, Nature 187 (4740) (1960) 869–870.
[2] Y. Sun, S.X. Peng, Q. Yang, F. Zhang, H.B. Yu, Predicting complex relaxation processes in metallic glass, Phys. Rev. Lett. 123 (10) (2019), 105701.
[3] M.X. Xia, S.G. Zhang, H.W. Wang, J.G. Li, The effect of Cu on the properties of Nd-based bulk metallic glasses, Mater. Des. 30 (4) (2009) 1236–1239.
[4] C. Zhang, W. Wang, Y.C. Li, Y.G. Yang, Y. Wu, L. Liu, 3D printing of Fe-based bulk metallic glasses and composites with large dimensions and enhanced toughness by thermal spraying, J. Mater. Chem. A 6 (16) (2018) 6800–6805.
[5] W.H. Wang, C. Dong, C.H. Shek, Bulk metallic glasses, Mater. Sci. Eng. R-Rep. 44 (2–3) (2004) 45–89.
[6] Z.L. Ning, W.Z. Liang, M.X. Zhang, Z.Z. Li, J.F. Sun, High tensile plasticity and strength of a CuZr-based bulk metallic glass composite, Mater. Des. 90 (2016) 145–150.
[7] J. Pan, Y.X. Wang, Q. Guo, D. Zhang, A.L. Greer, Y. Li, Extreme rejuvenation and softening in a bulk metallic glass, Nat. Commun. 9 (1) (2018) 1–9.
[8] G. Ji, S. Min, N. Song, G. Sheng, H. Yue, Effects of annealing on the hardness and elastic modulus of a $Cu_{36}Zr_{48}Al_8Ag_8$ bulk metallic glass, Mater. Des. 47 (2013) 706–710.
[9] C.J. Byrne, M. Eldrup, Materials science: bulk metallic glasses, Science 321 (5888) (2018) 502–503.
[10] Y. Wu, D. Ma, Q.K. Li, A.D. Stoica, W.L. Song, H. Wang, X.J. Liu, G.M. Stoica, G.Y. Wang, K. An, X.L. Wang, M. Li, Z.P. Lu, Transformation-induced plasticity in bulk metallic glass composites evidenced by in-situ neutron diffraction, Acta Mater. 124 (2017) 478–488.
[11] D. Zhou, B.J. Li, S.Y. Zhang, B. Hou, Y.L. Li, Rate-dependent shear banding and fracture behavior in a ductile bulk metallic glass, Mater. Sci. Eng. A 730 (2018) 270–279.
[12] P.Y. Li, Effects of strain rates on shear band and serrated flow in a bulk metallic glass, J. Non-Cryst. Solids 484 (2018) 30–35.
[13] A. Das, P. Kagebein, S. Kuchemann, R. Maass, Temperature rise from fracture in a Zr-based metallic glass, Appl. Phys. Lett. 112 (2018) 261905.
[14] N. Li, W. Chen, L. Liu, Thermoplastic micro-forming of bulk metallic glasses: a review, JOM 68 (4) (2016) 1246–1261.
[15] S. Bera, B. Sarac, S. Balakin, P. Ramasamy, M. Stoica, M. Calin, J. Eckert, Micropatterning by thermoplastic forming of Ni-free Ti-based bulk metallic glasses, Mater. Des. 120 (2017) 204–211.
[16] B. Bochtler, M. Stolpe, B. Reiplinger, R. Busch, Consolidation of amorphous powder by thermoplastic forming and subsequent mechanical testing, Mater. Des. 140 (2018) 188–195.
[17] S.M. Song, Y.C. Liao, T.H. Li, C.K. Lee, P.H. Tsai, J.S.C. Jang, J.C. Huang, Thermoplastic deformation behavior of a Fe-based bulk metallic glass within the supercooled liquid region, J. Mater. Res. Tech. 8 (2) (2019) 1907–1914.
[18] B.Y. Joo, S.H. Rhim, S.I. Oh, Micro-hole fabrication by mechanical punching process, J. Mater. Process. Tech. 170 (3) (2005) 593–601.
[19] T. Sano, M. Takahashi, Y. Murakoshi, K. Matsuno, H. Takeishi, Punchless blanking of an amorphous alloy, J. Mater. Process. Tech. 30 (3) (1992) 341–350.
[20] Y. Murakoshi, M. Takahashi, M. Terasaki, T. Sano, K. Matsuno, H. Takeishi, High-speed blanking of an amorphous alloy, J. Mater. Process. Tech. 30 (3) (1992) 329–339.
[21] Y. Huang, D. Wang, H. Fan, J. Sun, J. Shen, J. Mi, Shear punching of a Ti-based bulk metallic glass, Mater. Sci. Eng. A 561 (2013) 220–225.
[22] H. Li, Y. Yan, F. Sun, K. Li, F. Luo, J. Ma, Shear punching of amorphous alloys under high-frequency vibrations, Metals 9 (11) (2019) 1158.
[23] F. Takahashi, T. Nishimura, I. Suzuki, H. Kudo, A method of blanking from amorphous alloy foils using rubber tool, Cirp Ann-Manuf. Tech. 40 (1) (1991) 315–318.
[24] J.W. Qiao, H.Y. Ye, H.J. Yang, W. Liang, B.S. Xu, P.K. Liaw, M.W. Chen, Dynamic shear punching of metallic glass matrix composites, Intermetallics 36 (2013) 31–35.
[25] L.S. Huo, J. Ma, H.B. Ke, H.Y. Bai, D.Q. Zhao, W.H. Wang, The deformation units in metallic glasses revealed by stress-induced localized glass transition, J. Appl. Phys. 111 (11) (2012), 113522.
[26] J.C. Ye, J. Lu, C.T. Liu, Q. Wang, Y. Yang, Atomistic free-volume zones and inelastic deformation of metallic glasses, Nat. Mater. 9 (8) (2010) 619–623.
[27] Z. Wang, P. Wen, L.S. Huo, H.Y. Bai, W.H. Wang, Signature of viscous flow units in apparent elastic regime of metallic glasses, Appl. Phys. Lett. 101 (12) (2012) 121906.
[28] F. Luo, F. Sun, K. Li, F. Gong, X. Liang, X. Wu, J. Ma, Ultrasonic assisted micro-shear punching of amorphous alloy, Mater. Res. Lett. 6 (10) (2018) 545–551.
[29] P. Lunkenheimer, U. Schneider, R. Brand, A. Loid, Glassy dynamics, Contemp. Phys. 41 (1) (2000) 15–36.
[30] T. Egami, Atomic level stresses, Prog. Mater. Sci. 56 (6) (2011) 637–653.
[31] W. Liao, J. Hu, Y. Zhang, Micro forming and deformation behaviors of $Zr_{50.5}Cu_{27.45}Ni_{13.05}Al_9$ amorphous wires, Intermetallics 20 (1) (2012) 82–86.
[32] M. Geiger, F. Vollertsen, R. Kals, Fundamentals on the manufacturing of sheet metal microparts, Cirp Ann-Manuf. Techn. 45 (1) (1996) 277–282.
[33] X.K. Xi, D.Q. Zhao, M.X. Pan, W.H. Wang, Y. Wu, J.J. Lewandowski, Fracture of brittle metallic glasses: brittleness or plasticity, Phys. Rev. Lett. 94 (12) (2005), 125510.
[34] R.K. Guduru, K.A. Darling, R.O. Scattergood, C.C. Koch, K.L. Murty, M. Bakkal, A.J. Shih, Shear punch tests for a bulk metallic glass, Intermetallics 14 (12) (2006) 1411–1416.
[35] X. Huang, K.J. Hanley, Z. Zhang, C.Y. Kwok, Structural degradation of sands during cyclic liquefaction: insight from DEM simulations, Comput. Geotech. 114 (2019), 103139.

[36] J.A. Yamamuro, K.M. Covert, Monotonic and cyclic liquefaction of very loose sands with high silt content, J. Geotech. Geoenviron. 127 (4) (2001) 314–324.
[37] V.A. Khonik, V.M. Mikhailov, On the nature of homogeneous-inhomogeneous flow transition in metallic glasses: acoustic emission analysis, Scripta mater. 37 (3) (1997) 377–383.
[38] P. Zhang, J.J. Maldonis, Z. Liu, J. Schroers, P.M. Voyles, Spatially heterogeneous dynamics in a metallic glass forming liquid imaged by electron correlation microscopy, Nat. Commun. 9 (1) (2018) 1–7.
[39] C. Stern, A. Frick, G. Weickert, Relationship between the structure and mechanical properties of polypropylene: effects of the molecular weight and shear-induced structure, J. Appl. Polym. Sci. 103 (1) (2007) 519–533.
[40] Q.P. Sun, K.C. Hwang, S.W. Yu, A micromechanics constitutive model of transformation plasticity with shear and dilatation effect, J. Mech. Phys. Solids 39 (4) (1991) 507–524.
[41] J. Luo, Y. Shi, C.R. Picu, Shear-induced volumetric strain in CuZr metallic glass, Int. J. Eng. Sci. 83 (2014) 99–106.
[42] Y.J. Wang, M.Q. Jiang, Z.L. Tian, L.H. Dai, Direct atomic-scale evidence for shear-dilatation correlation in metallic glasses, Scripta Mater 112 (2016) 37–41.
[43] H.B. Ke, P. Wen, H.L. Peng, W.H. Wang, A.L. Greer, Homogeneous deformation of metallic glass at room temperature reveals large dilatation, Scripta Mater 64 (10) (2011) 966–969.
[44] C.X. Peng, D. Şopu, Y. Cheng, K.K. Song, S.H.W. ang, J. Eckert, L. Wang, Deformation behavior of designed dual-phase CuZr metallic glasses, Mater. Des. 168 (15) (2019) 107662.
[45] X.H. Sun, Y.S. Wang, J. Fan, H.J. Yang, S.G. Ma, Z.H. Wang, J.W. Qiao, Plasticity improvement for dendrite/metallic glass matrix composites by pre-deformation, Mater. Des. 86 (5) (2015) 266–271.